Mem. S.A.It. Vol. 83, 1128
© SAIt 2012
Memorie della

Gas accretion in distant galaxies as the origin of chemical abundance gradients

G. Cresci

Istituto Nazionale di Astrofisica – Osservatorio Astrofisico di Arcetri, Largo E. Fermi 5, I-50125, Firenze, Italy, e-mail: gcresci@arcetri.astro.it

Abstract. The metal content in galaxies provides important information on the physical processes responsible for galaxy formation, but little was known for galaxies at $z > 3$, when the Universe was less than 15% of its current age. We report on our metallicity survey of galaxies at $z > 3$ using SINFONI at the VLT. We find that a mass-metallicity relation is already established at $z \sim 3$, but we derive a significant evolution with respect to lower redshifts. In some of these massive galaxies we can even map the gas metallicity. In particular, we find a sample of galaxies at $z \sim 3.3$ showing regular rotation, though highly turbulent, and inverted abundance gradients relative to local galaxies, with lower metallicities close to the most active regions of star formation. We also find that at $z > 3$ the galaxies deviate from the fundamental relation between metallicity, mass and star formation rate defined by $0 < z < 2.5$ galaxies. Overall the results suggest that prominent inflow of pristine gas is responsible for the strong chemical evolution observed in galaxies at $z > 3$.

1. Introduction

Gas metallicity is regulated by a complex interplay between star formation, infall of metal-poor gas and outflow of enriched material. These concurrent phenomena are shaping the well known relation between stellar mass $M_\star$ and metallicity (McClure & van den Bergh 1968; Lequeux et al. 1979; Garnett 2002; Tremonti et al. 2004; Lee et al. 2006), with more massive galaxies showing higher metallicities. This mass-metallicity relation has also been studied in the early Universe, e.g. by Cresci et al. (2012) at $z \sim 0.6$, Savaglio et al. (2005) at $z \sim 0.8$, Queyrel et al. (2012) at $z \sim 1.5$, and by Erb et al. (2006) at z∼2.2, finding a strong and monotonic evolution, with metallicity decreasing with redshift at a given mass (see Fig.1).

Until recently, little was known about the metallicity of galaxies at $z > 3$, due to the difficulty of detecting the optical nebular lines (redshifted into the near-infrared) required to measure the metallicity in these faint systems. However, this is a crucial epoch of very fast galaxy evolution, just before the peak of cosmic star formation, which requires detailed investigation to understand the formation of primeval galaxies.

2. AMAZE and LSD

Integral field imaging spectroscopy is a unique tool to directly probe the mass assembly in the crucial epochs of galaxy evolution. In this context, we have recently begun a study of two samples of $z > 3$ star forming galaxies, 1 Gyr after the Big Bang, selected on the basis of their rest-frame ultra-violet/optical colours

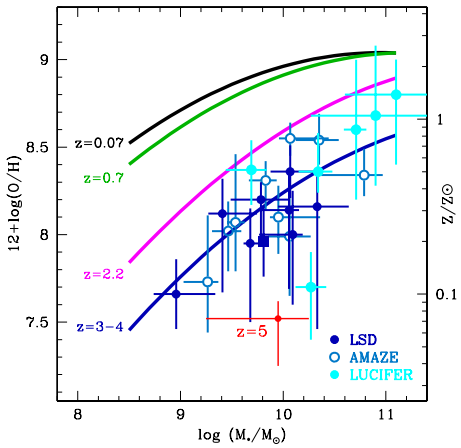

Fig. 1. Evolution of the mass-metallicity relation from local to high redshift galaxies. Data are from Kewley & Ellison (2008) (z=0.07), Savaglio et al. (2005) (z=0.7), Erb et al. (2006) (z=2.2), Mannucci et al. (2009) and Cresci et al. (in preparation, z=3–5).

with the Lyman-break technique. The galaxies have been observed with the near-infrared integral field spectrometer SINFONI on the Very Large Telescope of the European Southern Observatory. These two projects, AMAZE (Maiolino et al. 2008) and LSD (Mannucci et al. 2009) were aimed at the exploration of chemical and dynamical evolution of galaxies beyond $z \sim 3$.

For AMAZE, described in Maiolino et al. (2008), we selected 30 UV selected $z = 3 - 5$ galaxies with deep Spitzer/Infrared Array Camera (IRAC) photometry ($3.6 - 8\mu m$), an important piece of information to derive a reliable stellar mass. These galaxies were observed with SINFONI in seeing limited mode. On the other hand, we observed in the LSD survey, described in Mannucci et al. (2009), a sample of 10 Lyman-Break Galaxies at $z \sim 3$ from the Steidel et al. (2003) catalog. The parent sample was searched for the presence of bright stars ($R < 15$) within $\sim 35''$ from the target, in order to improve the spatial resolution up to $\sim 0.1 - 0.2''$ thanks to Natural Guide Star adaptive optics (AO). No other property was used to select the targets, thus the sample, albeit small, should be representative of the LBG population in the Steidel et al. (2003) population.

Moreover, we have an ongoing project to observe $\sim$ 40 additional $z \sim 3$ galaxies from the Steidel et al. (2003) sample in four fields with the multi-object near-IR spectrometer LUCI1 at the LBT. Galaxy (projected) overdensities have been selected in order to maximize the number of targets for MOS observations, providing $\sim$ 10 objects per field in the LUCI1 field of view ($4' \times 4'$). The observations are still ongoing, although the data for the first field are completed, providing the spectra of 6 additional galaxies.

Metallicity at z~3 can be measured from the line flux ratios of [OIII]λ4958,5007, [OII]λ3727 [NeIII] and Hβ (see Maiolino et al. 2008), while SFR is derived from the flux of Hβ corrected for dust extinction and the stellar masses from SED fitting using photometric data from the optical to the mid-IR (see Mannucci et al. 2009). Fig. 1 shows the stellar mass-metallicity relation at $z \sim 3$, compared to the same relation as measured at lower redshifts. All the presented data have been scaled to a Chabrier (2003) IMF and use the same metallicity calibration. A strong, monotonic evolution of metallicity can be seen, i.e. galaxies at $z \sim 3$ have metallicities about six times lower than galaxies of similar stellar mass in the local universe.

3. Metallicity gradients in $z \sim 3$ galaxies

The results discussed so far made use of gas phase metallicities derived from line ratios integrated over the entire galaxies. However, the quality of the integral field spectroscopy for the brightest and most extended sources in AMAZE and LSD is good enough to study the chemical properties of their single spatially-resolved regions, and investigate the presence of metallicity variations across the galaxies.

The existence of prominent metallicity gradients is now well established in several local galaxies (Garnett 2002), including our own (Magrini et al. 2009). Various chemio-dynamical models have been proposed to ex-

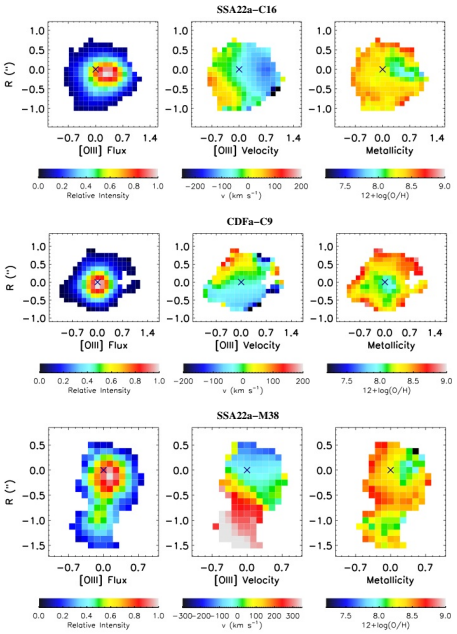

Fig. 2. Surface brightness of the [OIII]λ5007 line, velocity map, and gas phase metallicity, plotted as relative abundances of oxygen and hydrogen parameterized in units of $12+log(O/H)$, of the three galaxies in Cresci et al. (2010). Lower metallicity region are surrounded by a more enriched disk. The crosses in each panel mark the position of the continuum peak.

plain the observed variations in the abundances of elements (Molla et al. 1997; Hou et al. 2000; Chiappini et al. 2001). Generally, metallicity gradients are strongly influenced by the effect of concurrent phenomena, like accretion of metal-poor gas from the halo, radially dependent formation of new stars that enrich the pre-existing gas, outflows ejecting metal-enriched gas out of the galaxies, and redistribution of mass within galaxies, such as via clump migration/disruption (Immeli et al. 2004) or mixing due to a stellar bar. All these factors have profound implications on the global evolution of galaxies, making it crucial to understand their relative roles. The investigation of metallicity gradients is therefore a unique tool to reveal the physical mechanisms behind the formation and evolution of galaxies. This is even more important for galaxies at the earliest stages of their evolution, where the differences expected from different models are the largest.

To test the for the presence of abundances gradients in our $z \sim 3$ sample, we selected three Lyman-break galaxies among the AMAZE (Maiolino et al. 2008) and LSD (Mannucci et al. 2009) samples which show a remarkably symmetric velocity field in the [OIII] emission line, which traces the ionized gas kinematics (see Fig. 3). Such kinematics indicates that these are rotationally supported disks (see Gnerucci et al. 2011), with no evidence for more complex merger-induced dynamics. We used the flux ratios between the main rest-frame optical lines to obtain the metallicity map shown in Fig. 3 (Cresci et al. 2010). An unresolved region with lower metallicity is evident in each map, surrounded by a more uniform disk of higher metal content. In one case, CDFa-C9, the lower metallicity region is coincident with the galaxy center, as traced by the continuum peak, while it is offset by $\sim 0.60''$ (4.6 kpc) in SS22a-C16 and $\sim 0.45''$ (3.4 kpc) in SS22a-M38. On the other hand, in all the galaxies the area of lower metallicity is coincident or closer than $0.25''$ (1.9 kpc, half of the PSF FWHM) to the regions of enhanced line emission, tracing the more active star forming regions. The average difference between high and low metallicity regions in the three galaxies is 0.55 in units of 12+log(O/H), larger than the $\sim 0.2 - 0.4$ dex gradients measured in the Milky Way and other local spirals (van Zee et al. 1998) on the same spatial scales. The measured gas phase abundance variations have a significance between 98% and 99.8% . It can be shown (Cresci et al. 2010) that variations of ionization parameter across the galaxies cannot explain the observed gradients of line ratios, and that different metallicities are really required.

The detected gradients can be explained in the framework of the cold gas accretion scenario (Kereš et al. 2005) recently proposed to explain the properties of gas rich, rotationally supported galaxies observed at high redshift (Cresci et al. 2009; Forster Schreiber et al. 2009). In this scenario, the observed low metallicity regions are created by the local accretion of metal-poor gas in clumpy streams (Dekel

et al. 2009), penetrating deep onto the galaxy following the potential well, and sustaining the observed high star formation rate in the pre-enriched disk. Stream-driven turbulence is then responsible for the fragmentation of the disks into giant clumps, as observed at $z \geq 2$ (Genzel et al. 2008; Mannucci et al. 2009), that are the sites of efficient star formation and possibly the progenitors of the central spheroid. This scenario is also in agreement with the dynamical properties of our sample, which appears to be dominated by gas rotation in a disk with no evidence of the dynamical asymmetries typically induced by mergers. The study of the relations between metallicity gas fractions, effective yields, and SFR (Cresci et al. 2010) shows that the low-metallicity regions can be well explained by amounts of infalling gas much larger than in the remaining high-metallicity regions.

Recent models of chemical enrichment in galaxies (Chiappini et al. 2001, Curir et al. (2012), Matteucci et al. in prep) are actually predicting "inverse" gradients at high redshift in the framework of the "inside-out" formation scenario for disk galaxies, and explain the positive rotation-metallicity correlation of the old thick disk population as the relic signature of an ancient "inverse" chemical (radial) gradient in the inner Galaxy, which resulted from accretion of primordial gas at $z \sim 3-4$.

Our observations of low metallicity regions in these three galaxies at $z \sim 3$ therefore provide the evidence for the actual presence of accretion of metal-poor gas in massive high-z galaxies, capable to sustain high star formation rates without frequent mergers of already evolved and enriched sub-units. This picture is also in agreement with discovery of a close relation between SFR, stellar mass and metallicity in star forming galaxies.

4. The Fundamental Metallicity Relation

If infall is at the origin of the star formation activity, and outflows are produced by exploding supernovae (SNe), a relation between metallicity and SFR is likely to exist. In other words, SFR is a parameter that should be considered in the scaling relations that include metallicity, such as the mass-metallicity relation.

To test the hypothesis of a correlation between SFR and metallicity in the present universe and at high redshift, we have studied several samples of galaxies at different redshifts whose metallicity, $M_\star$, and SFR have been measured. A full description of the data sets and selection criteria used is given in Mannucci et al. (2010).

Local galaxies are well measured by the SDSS project (Abazajian et al. 2009), for which we found, at fixed mass, a systematic segregation in SFR in the mas-metallicity relation. While galaxies with high $M_\star$ ($\log(M_\star)>10.9$) show no correlation between metallicity and SFR, at low $M_\star$ more active galaxies also show lower metallicity.

The obtained dependence of metallicity on $M_\star$ and SFR can be visualized in a 3D space with these three coordinates, as shown in Figure 3. SDSS galaxies appear to define a tight surface in the space, the Fundamental Metallicity Relation (FMR). The introduction of the FMR results in a significant reduction of residual metallicity scatter with respect to the simple mass-metallicity relation. The dispersion of individual SDSS galaxies around the FMR, is ∼0.06 dex when computed across the full FMR and reduces to ∼0.05 dex i.e, about 12%, in the central part of the relation where most of the galaxies are found. The final scatter is consistent with the intrinsic uncertainties in the measure of metallicity (∼0.03 dex for the calibration, to be added to the uncertainties in the line ratios), on mass (estimated to be 0.09 dex by Tremonti et al. 2004), and on the SFR, which are dominated by the uncertainties on dust extinction.

The reduction in scatter with respect to the mass-metallicity relation becomes even more significant when considering that most of the galaxies in the sample cover a small range in SFR, with 64% of the galaxies ($\pm 1\sigma$) is contained inside 0.8 dex. The mass-metallicity relation is not an adequate representation of galaxy samples with a larger spread of SFRs, as usually find at intermediate redshifts.

We therefore compared the relation defined by local galaxies with several samples

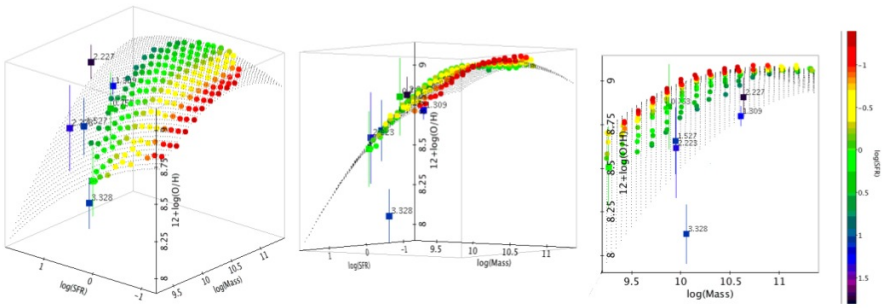

Fig. 3. Three projections of the Fundamental Metallicity Relation among $M_\star$, SFR and gas-phase metallicity. Circles without error bars are the median values of metallicity of local SDSS galaxies in bin of $M_\star$ and SFR, color-coded with SFR as shown in the colorbar on the right. These galaxies define a tight surface in the 3D space, with dispersion of single galaxies around this surface of ∼0.05 dex. The black dots show a second-order fit to these SDSS data, extrapolated toward higher SFR. Square dots with error bars are the median values of high redshift galaxies, as explained in the text. Labels show the corresponding redshifts. The projection in the center emphasizes that most of the high-redshift data, except the point at z=3.3, are found on the same surface defined by low-redshift data. The projection on the right correspond to the mass-metallicity relation, showing that the origin of the observed evolution in metallicity up to $z \sim 2.5$ is due to progressively increasing SFR.

of high-redshift objects. We extracted from the literature samples of galaxies in four redshift bins, for a total of ∼300 objects, having published values of emission line fluxes, $M_\star$, and dust extinction: 0.5<z<0.9 (Savaglio et al. (2005), GDDS galaxies, Cresci et al. (2012), COSMOS galaxies), 1.0<z<1.6 (Shapley et al. 2005; Liu et al. 2008; Wright et al. 2009; Epinat et al. 2009), 2.0<z<2.5 (Erb et al. 2006; Law et al. 2009; Lehnert et al. 2009; Forster Schreiber et al. 2009), and 3.0<z<3.7 (Maiolino et al. 2008; Mannucci et al. 2009).

Median values of $M_\star$, SFR and metallicities in two different mass bins were computed for each of these samples.

Galaxies up to z∼2.5 follow the FMR defined locally, with no sign of evolution. This is an unexpected result, as simultaneously the mass-metallicity relation is observed to evolve rapidly with redshift (see Fig.1). The solution of this apparent paradox is that distant galaxies have, on average, larger SFRs, and, therefore, fall in a different part of the same FMR.

However, galaxies at z∼3.3 show metallicities lower of about 0.6 dex with respect to both the FMR defined by the SDSS sample and galaxies at 0.5<z<2.5. This is an indication that some evolution of the FMR appears at z>2.5, although its size can be affected several potential biases (see Mannucci et al. (2010) and Troncoso et al. in preparation for a full discussion). A larger data set at z>3 is needed to answer this question.

5. Conclusions

The interpretation of these results must take into account several effects. In principle, metallicity is a simple quantity as it is dominated by three processes: star formation, infall, outflow. If the scaling laws of each of these three processes are known, the dependence of metallicity on SFR and $M_\star$ can be predicted. In practice, these three processes have a very complex dependence on the properties of the galaxies, and can introduce scaling relations in many different ways. The conditions for the existence of the FMR and the observation of ”inverted” metallicity gradients at high-z fit into the smooth accretion models proposed by several groups (Bournaud & Elmegreen 2009; Dekel et al. 2009), where continuos infall of pristine gas is the main driver of the grow of galaxies. In this case, metal-poor gas is contin-

uously accreted by galaxies and converted in stars, and a long-lasting equilibrium between gas accretion, star formation, and metal ejection is expected to established. However, detailed observations of larger samples of galaxies,especially at $z > 3$ are needed to finally understand the main mechanisms regulating galaxy growth and chemical enrichment at high redshift: the forthcoming generation of telescopes (e.g. ELT and JWST) and instruments (e.g. KMOS@VLT) will finally provide the higher sensitivity and larger semples required to significantly improve our understanding of metal enrichment in the early Universe.

References

Abazajian, K. N., et al. 2009, ApJS, 182, 543
Bournaud, F. & Elmegreen, B. G. 2009, ApJL, 694, L158
Chabrier, G. 2003, PASP, 115, 763
Chiappini, C., Matteucci, F., & Romano, D. 2001, ApJ, 554, 1044
Cresci, G., et al. 2009, ApJ, 697, 115
Cresci, G., et al. 2010, Nature, 467, 811
Cresci, G., et al. 2012, MNRAS, 421, 262
Curir, A., et al. 2012, A&A, 545, A133
Dekel, A., Sari, R., & Ceverino, D. 2009, ApJ, 703, 785
Epinat, B., et al. 2009, A&A, 504, 789
Erb, D. K., et al. 2006, ApJ, 644, 813
F″orster Schreiber, N. M., et al. 2009, ApJ, 706, 1364
Garnett, D. R. 2002, ApJ, 581, 1019
Genzel, R., et al. 2008, ApJ, 687, 59
Gnerucci, A., et al. 2011, A&A, 528, A88
Hou, J. L., Prantzos, N., & Boissier, S., 2000, A&A, 362, 921
Immeli, A., Samland, M., Westera, P., & Gerhard, O. 2004, ApJ, 611, 20
Kauffmann, G., et al. 2003, MNRAS, 341, 33
Kennicutt, Jr., R. C. 1998, ARAA, 36, 189
Kereš, D., Katz, N., Weinberg, D. H., & Dave, R. 2005, MNRAS, 363, 2
Kewley, L. J. & Ellison, S. L. 2008, ApJ, 681, 1183
Law, D. R., et al. 2009, ApJ, 697, 2057
Lee, H., et al. 2006, ApJ, 647, 970
Lehnert, M. D., et al. 2009, ApJ, 699, 1660
Lequeux, J., et al. 1979, A&A, 80, 155
Liu, X., et al. 2008, ApJ, 678, 758
Magrini, L., Sestito, P., Randich, S., & Galli, D., 2009, A&A, 494, 95
Maiolino, R., et al. 2008, A&A, 488, 463
Mannucci, F., et al. 2009, MNRAS, 398, 1915
Mannucci, F., et al. 2010, MNRAS, 408, 2115
McClure, R. D. & van den Bergh, S. 1968, AJ, 73, 1008
Molla, M., Ferrini, F., & Diaz, A. I. 1997, ApJ, 475, 519
Mouchine, M., Gibson, B. K., Renda, A., & Kawata, D. 2008, ArXiv e-prints
Queyrel, J., Contini, T., Kissler-Patig, M., et al. 2012, A&A, 539, A93
Savaglio, S., et al. 2005, ApJ, 635, 260
Shapley, A. E., Coil, A. L., Ma, C.-P., & Bundy, K. 2005, ApJ, 635, 1006
Steidel, C. C., et al. 2003, ApJ, 592, 728
Tremonti, C. A., et al. 2004, ApJ, 613, 898
van Zee, L., et al. 1998, AJ, 116, 2805
Wright, S. A., et al. 2009, ApJ, 699, 421